

ANALYSIS OF TURMERIC (*CURCUMA LONGA* LINN) ESSENTIAL OIL FROM DIFFERENT GROWING LOCATIONS USING FTIR/GC-MS SPECTROSCOPY COUPLED TO CHEMOMETRICS AND ITS WOUND HEALING ACTIVITIES

SURYATI SYAFRI¹, RISKANA SORAYA PUTRI², IRWANDI JASWIR³, FARIDAH YUSOF⁴, YOHANNES ALEN⁵, SYOFYAN SYOFYAN⁶, DACHRIYANUS HAMIDI^{7*}

^{1,2,5,7}Department of Pharmaceutical Biology, Faculty of Pharmacy. Universitas Andalas. Padang. West Sumatera, Indonesia. ³International Institute of Halal Research and Training. International Islamic University Malaysia. ⁴Departement of Biotechnology Engineering. Kulliyah of Engineering International Islamic University Malaysia. ⁶Department of Pharmaceutical Technology, Faculty of Pharmacy. Universitas Andalas. Padang. West Sumatera, Indonesia

*Corresponding author: Dachriyanus Hamidi; *Email: dachriyanus@phar.unand.ac.id

Received: 14 Oct 2023, Revised and Accepted: 23 Nov 2023

ABSTRACT

Objective: This study aims to determine the wound-healing activity of turmeric essential oil (TEO) collected from seven growing locations in West Sumatra, classify it based on fingerprint patterns of IR spectra combined with chemometrics, and identify their metabolite profiling using GC-MS spectroscopy.

Methods: Fresh turmeric rhizome was extracted by the hydrodistillation method. TEO classification was carried out by PCA (Principal Component Analysis), and PLS-DA (Partial Least Squares-Discriminant Analysis) was used for predicting characteristic functional groups and metabolites (VIP>1) in TEO. Wound healing activity was performed using *in vitro* fibroblast cell proliferation and migration assay. Data analysis was performed using one-way ANOVA with a 95% confidence level.

Results: PCA analysis based FTIR spectra was able to determine highland and lowland-originated TEO. The metabolites responsible for TEO classification were α -Phellandrene and D-limonene. The result showed that TEO originating from both lowlands and highlands enhanced fibroblast cell proliferation and fibroblast cell migration.

Conclusion: The combination of IR spectral fingerprint patterns and chemometric analysis could classify TEO based on the height location of growth. The results showed that the altitude of the growing location had no significant effect on the wound-healing activity of TEO from West Sumatra ($p>0.05$).

Keywords: Turmeric, Essential oil, FTIR, GC-MS, Chemometrics, Wound healing

© 2024 The Authors. Published by Innovare Academic Sciences Pvt.Ltd. This is an open access article under the CC BY license (<https://creativecommons.org/licenses/by/4.0/>) DOI: <https://dx.doi.org/10.22159/ijap.2024.v16s1.33> Journal homepage: <https://innovareacademics.in/journals/index.php/ijap>

INTRODUCTION

The development of wound medicine or “wound dressings” for acute and chronic wounds is still a global challenge; even though treatments for wounds are available, such as surgery, autografts, topical dressings, corticosteroids, laser therapy, and topical therapeutic agents, the management of wounds and chronic pain in patients burns still unsatisfactory [1]. Furthermore, treatment of wounds using synthetic drugs can cause unwanted side effects such as skin hypersensitivity reactions and even cause hyperthyroidism [2]. Therefore, there is a need to find effective treatments with low side effects. Wound healing is a dynamic process after a skin injury, starting from inflammation, proliferation, and migration of several types of cells, such as fibroblasts and the remodeling phase. Fibroblast cells have an important role in tissue repair, starting from the final stage of inflammation to the formation of epithelial cells in injured tissues by secreting growth factors, cytokines, collagen, and other extracellular matrix components [3]. Fibroblast proliferation in the wound healing process is naturally stimulated by interleukin-1b (IL-1b), platelet-derived growth factor (PDGF), and fibroblast growth factor (FGF). In addition, the migration of fibroblasts to the damaged area is stimulated by the transforming growth factor (TGF), which is a growth factor produced by granulation tissue formed during the inflammatory process [4, 5].

The search for more effective drug sources for wound healing and cost-effectiveness is still ongoing. Bioactive products extracted from plants are an attractive source for developing new drugs because plants are an inexhaustible source of active substances [6]. Turmeric rhizomes contain an essential oil which rich in terpenoids compounds. Studies have demonstrated that terpenoid compounds

can promote wound healing by exhibiting astringent and antimicrobial properties. These properties are believed to contribute to wound contraction and facilitate faster epithelialization [7]. However, the biological activity of essential oils is greatly influenced by their chemical composition, which can be affected by several factors, including light exposure, geographical location, amount of rainfall, and soil quality [8].

West Sumatra is a province in Indonesia situated on the west coast of the central part of Sumatra Island. The region comprises lowlands on the west coast and volcanic plateaus formed by the Bukit Barisan on the eastern side. West Sumatra is known for its abundant medicinal plants, both growing wild and in plantations, including the Zingiberaceae family [9, 10]. Although many studies have been carried out on turmeric essential oil, there was a lack of research on the wound-healing activity of turmeric rhizome that grows in West Sumatra. Therefore, this research aims to identify metabolite profiling turmeric essential oil from seven different locations in West Sumatra using FTIR and GC-MS spectroscopies coupled to chemometrics and evaluate their wound healing activity.

MATERIALS AND METHODS

Plant collection

Turmeric rhizomes were harvested from seven distinct districts of West Sumatra, Indonesia. Beginning in September 2022: Pasaman Barat (PB), Solok (SO), Pesisir Selatan (PS), Sijunjung (SJ), Dharmasraya (DM), Agam (AG), and Padang Pariaman (PP) (fig. 1). The following table 1 describes the geographical condition for each location.

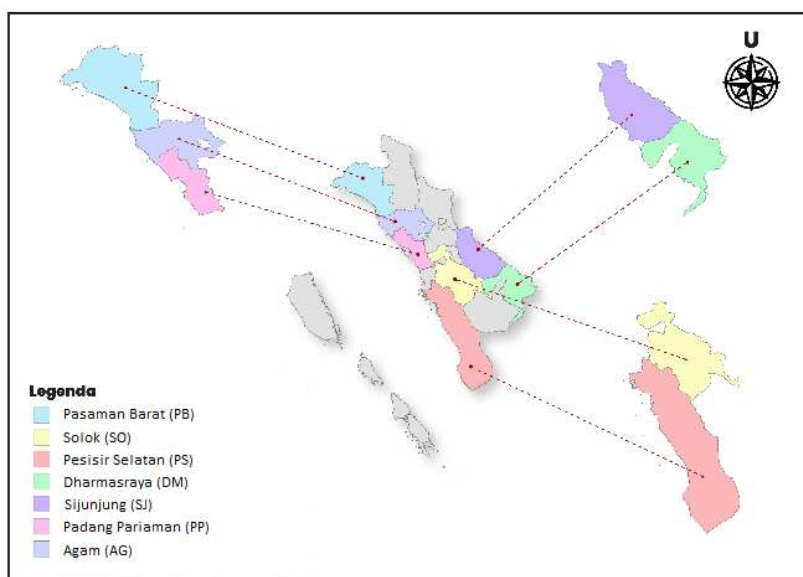


Fig. 1: Geographical location of turmeric EOs origin

Table 1: Geographical condition

Location	Altitude (m)	Code	Coordinate	Temp (°C)	Humidity
Kinali, Pasaman Barat	30 m	PB	0°3'17"S 99°54'14"E	25	91%
Gunung Talang, Solok	1094 m	SO	0°58'46"S 100°37'18"E	21	90%
Lunang, Pesisir Selatan	24 m	PS	2°16'25"S 101°8'35"E	25	90%
Sitiung, Dharmasraya	94 m	DM	1°1'52"S 101°37'14"E	26	85%
Lubuk Tarok, Sijunjung	162 m	SJ	0°42'13"S 100°58'38"E	25	86%
Batang Anai, Padang Pariaman	10 m	PP	0°44'12"S 100°15'42"E	26	87%
Kamang Magek, Agam	880 m	AG	0°15'30"S 100°24'32"E	21	89%

Essential oil extraction

The fresh rhizomes were washed and sorted with tapped water before being cut and put to a distillation flask fitted with a Clevenger apparatus. The hydrodistillation procedure took around 8 h. The essential oils were collected in a dark bottle and Na_2SO_4 powder was used to remove any residual water. It was then stored at 4 °C until further usage [11]. The TEO was then evaluated for physical characterization, including yield, color, odor, specific gravity and refractive index.

ATR-FTIR spectrum measurement

The FTIR spectra were acquired using a (Shimadzu FTIR spectrometer). The sample was placed on the ATR (Smart iTR) surface and scanned in the MIR area with wavenumbers 4000-400

cm^{-1} at a controlled ambient temperature of 25 °C. It was examined with 32 scanners and a resolution of 8 cm^{-1} . The obtained spectra were automatically corrected or adjusted by using previously measured air as the background. The spectral measurements were done in triplicate. All of the resulting spectra were pre-processed, including atmospheric correction and smoothing.

Analysis of essential oils using gas chromatography-mass spectrometry (GC-MS)

GC-MS Gas Chromatography-Mass Spectrometry (Shimadzu GCMS-QP 2010 SE) and an RTX1 column were used to analyze essential oil under the following conditions (table 2). The compound was identified using the "WILEY library" included in the GC-MS program by analyzing fragmentation patterns from previously reported articles and the NIST Chemistry Webbook. SRD 69.

Table 2: The GC-MS condition

Parameter	Condition
GC Condition Inlet	
Heater	250 °C
Pressure	11.7 psi
Split ratio	200: 1
Split flow	240 ml/min
Columns	RTX-1
Flow rate	1.2 ml/min
Pressure	11.7 psi
Oven	Initial temperature: 80 °C
	Initial time: 1 min
Temperature program	80-110 °C at a rate 2 °C/min. 110-140 °C at a rate 3 °C/min. 140-170 °C at a rate 4 °C/min. 170-200 °C at a rate 5 °C/min
MS Condition	MS Source: 230 °C
	MS Quad: 150 °C
	Tune type: EI

Chemometric analysis

Chemometric analysis was performed using SIMCA application version 14.1 for both FT-IR and GC-MS spectra. Before chemometric analysis, the FTIR spectra were preprocessed by atmospheric correction using OMNIC software 1. For the classification of TEO, the data were analyzed using PCA (Principal Component Analysis), and PLS-DA was performed to identify the constituents influencing the classification.

Primary culture of fibroblast cell

Fibroblast cells were obtained from the fetal muscle of mice aged 10-14 d. The fetal body was carefully minced with a sterile knife, placed in a Falcon tube with 5 ml of phosphate-buffered saline (PBS), and spin for 5 min at 2000rpm. After removing the supernatant, 5 ml of PBS was added before spinning three times. Then 2 ml of 0,25% trypsin EDTA was incorporated and vortexed for a time. After 5 min, the falcon tube containing cells and PBS was placed in a 37 °C Water Bath. The medium, which supplemented with 10 ml of full RPMI (10% Fetal Bovine Serum+1% Penicillin-Streptomycin) was added and spin at 2000rpm for 5 min. Following the removal of the supernatant, 12 ml of full RPMI medium was added. Cell suspensions were cultivated in 6-well plates and maintained at 37 °C with 5% CO₂ for two days.

Fibroblast proliferation activity

The proliferation of fibroblast cell was carried out using the 3-(4,5)-dimethylthiaziazolo(-z-y1)-3,5 diphenyltetrazoliumbromide (MTT) assay method on a 96-well plate. Each well received 180 µl of fibroblast cell suspension (density of 10000 cells/well). The plate was incubated in a CO₂ incubator at 37 °C with 5% CO₂ for 24 h. The well was then filled with 20 µl of test sample with concentrations of 100; 10; 1; and 0,1 g/ml in DMSO. For the negative control, RPMI medium containing dimethyl sulfoxide (DMSO) was added to the well. The 96-well plates were then incubated in a CO₂ incubator at 37 °C with 5% CO₂ for 24-48 h. Following that, 100 µl MTT (0,5 mg/ml) was added to each well and incubated for 4-6 h at 37 °C with 5% CO₂. Purple formazan will develop when viable cells react. In 100

µl of DMSO, the produced formazan crystals were dissolved. The absorbance of each well was then measured at 550 nm using a microplate reader. The test was repeated three times. The percentage of fibroblast cell proliferation was calculated by formula:

$$\% \text{ Proliferation} = \frac{\text{Absorbance of samples}}{\text{Absorbance of control}} \times 100\%$$

Fibroblast cell migration using scratch assay

Fibroblast cells were cultivated in 24-well plates with 10⁵ cells per well until confluence was reached. The yellow tip was then used to make a straight wound. To remove cellular debris. Thoroughly rinse with 500 µl of Phosphate Buffer Saline (PBS). Then, 1 ml of each test solution (0,1 g/ml; 1 g/ml; and 10 g/ml in DMSO) was added to each well, with the exception of the control. Which received 1 ml of DMEM-containing solvent (DMSO). The experiment was repeated three times. The plate was incubated at 37 °C with 5% CO₂ in an incubator. Cell migration was then observed using an inverted microscope at 0; 24; and 48 h. The wound closure was calculated using the formula below:

$$\% \text{ Wound closure} = \frac{(\text{Areat0} - \text{Areat24/t48})}{\text{Areat0}} \times 100\%$$

Data analysis

The data analysis was performed using Minitab version 20 software. Using One-way ANOVA followed by Tukey analysis. Prior to data analysis, the data was examined to ensure that it was normally distributed. The p-value was significant at the 0.05.

RESULTS AND DISCUSSION

Physical characteristics

The physicochemical properties of oil reveal the essential oil's quality. Table 3 lists the physical properties of each essential oil, including yield, color, refractive index, specific gravity and optical rotation. Turmeric essential oil has a distinct smell and brown color. The obtained yield ranged from 0.179% w/v to more than 0.460% w/v. Fig. 2 displays TEOs color.

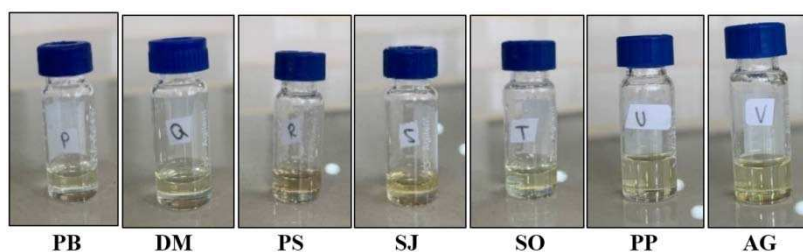


Fig. 2: Turmeric essential oil

Table 3: Physical characteristic of turmeric EOs

Sample	Physical characteristics			
	Yield (%v/v)	Colour	Specific gravity (g/ml)	Refractive index
PB	0.226	Pale yellow	0.92	1.511
SO	0.200	Pale yellow	0.94	1.513
PS	0.201	Brownish-yellow	0.98	1.516
DM	0.235	Pale yellow	0.92	1.510
SJ	0.179	Golden yellow	0.91	1.510
PP	0.216	Pale yellow	0.95	1.512
AG	0.460	Pale yellow	0.93	1.514

FTIR spectroscopy combined with chemometric analysis

FTIR fingerprinting was used to evaluate turmeric essential oil from seven different areas. In fig. 3 the FTIR spectra of TEO are displayed in the Middle Infra-Red (MIR) region. The spectra display the prominent peaks at 2,959-2,800 cm⁻¹ which are assigned to symmetric and

antisymmetric C-H stretching of alkane chain CH₂ and CH₃ groups. Additionally, the peak at 1684-1617 cm⁻¹ is due to C = C stretching. Methylene and methyl (C-H) bending vibrations can be observed at wavenumbers of 1445-1376 cm⁻¹. The peak at 1030-1117 cm⁻¹ is caused by C-O vibrations, while the bending out of plane vibrations of HC=CH (trans) and HC = CH (cis) appear at 988-841 cm⁻¹ [12, 13].

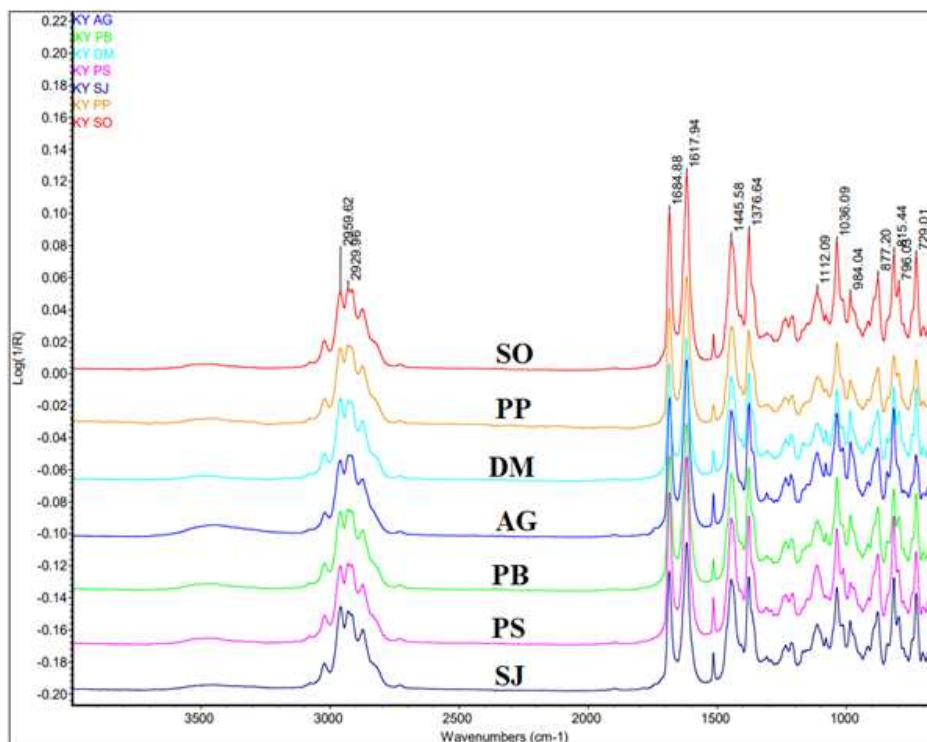


Fig. 3: FTIR spectra of turmeric Eos

The PCA (Principal Component Analysis) generates a score plot. In this study, the absorbance of wave numbers ranging from 2000-400 cm⁻¹ was analyzed using PCA and reduced to a principal component (PC) that could capture the structure and variation in the data [14]. The PCA scores plot below shows that PC-1 accounted for 72.8% and PC-2 accounted for 21.9%, so a total of 94.70 % in the PCA analysis

developed using six latent variables. After analyzing the score plot, it appears that TEO can be categorized into two distinct groups: lowland and highland. Highland covered a region more than 600 meters above sea level, whereby up to 600 meters above sea level was recognized as the lowland zone [15]. The lowland-originated TEO is distributed in the PC-1, while highland TEO is in the PC-2.

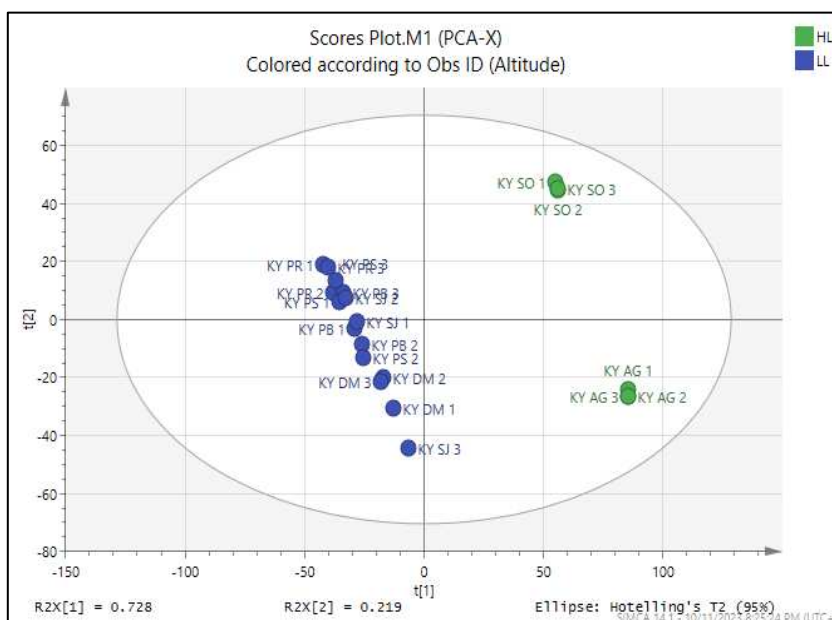


Fig. 4: PCA score plots for the main components (PC-1) and (PC-2) on all samples of turmeric EOs based on growing location

GC-MS analysis combined with chemometrics

The primary composition of turmeric EO from seven locations is described in table 4. The EOs have the same major compounds; however, the relative area percentage differed. B-Turmerone, Ar-

turmerone, Eucalyptol, and α-Phellandrene are the main constituent that characterizes Turmeric essential oil. The TEO from the highland had a higher percentage of β-Turmerone and eucalyptol. Otherwise, the higher percentage of Ar-turmerone in TEO originated from the lowlands.

Table 4: Chemical profiling of turmeric essential oils

Chemical component	Origin						
	AG	DM	SO	PS	SJ	PP	PB
α-Phellandrene	6.383	18.263	25.306	9.620	19.330	17.470	13.196
p-Cymene	3.674	4.642	0.000	0.000	0.000	0.000	0.000
Eucalyptol	11.484	7.858	12.760	2.061	6.112	8.877	6.936
Terpinolene	1.812	3.039	4.035	0.000	1.780	0.000	2.857
α-Curcumene	1.766	0.000	0.000	0.000	0.000	0.000	0.000
β-Sesquiphellandrene	1.286	0.000	1.863	0.000	0.000	0.000	0.000
ar-Turmerol	5.292	1.724	0.000	2.395	1.933	0.000	0.000
Eremophila-1(10).8.11-triene	2.948	0.000	0.000	1.873	0.000	0.000	0.000
1.4(15).11-Eudesmatriene	2.834	0.000	3.323	1.683	1.506	0.000	0.000
4-(2-Butyl)toluene	2.038	0.000	0.000	0.000	0.000	0.000	0.000
β-Farnesene	1.318	0.000	0.000	0.000	0.000	0.000	0.000
Ar-tumerone	14.474	32.988	15.549	41.448	34.367	61.004	71.060
Tricyclo[7.1.0.0[1.3]]decane-2-carbaldehyde	1.479	0.000	0.000	0.000	0.000	0.000	0.000
(E, E)-Germacrone	1.603	0.000	0.000	0.000	0.000	0.000	0.000
β-Turmerone	32.279	24.254	51.704	23.731	24.019	25.665	39.456
1-Bisabolone	1.443	0.000	0.000	0.000	0.000	0.000	0.000
Camphene	2.616	0.000	0.000	0.000	0.000	0.000	0.000
Thymyl angelate	2.679	0.000	0.000	1.286	0.000	0.000	0.000
β-Cymene	2.050	0.000	0.000	0.000	0.000	3.301	0.000
2-Pyrazoline. 1-allyl-	1.520	0.000	0.000	0.000	0.000	0.000	0.000
Pinocamphyl tiglate. iso-	1.692	0.000	0.000	1.050	0.000	0.000	0.000
Carveol acetate	4.318	0.000	0.000	0.000	0.000	0.000	0.000
D-Limonene	0.000	1.567	2.090	0.000	1.739	0.000	0.000
β-Curcumene	0.000	2.328	0.000	0.000	0.000	0.000	0.000
1-Buten-3-yne. 2-tert-butyl-	0.000	1.517	0.000	0.000	0.000	0.000	0.000
o-Cymene	0.000	0.000	6.307	2.520	6.401	0.000	0.000
Zingiberene	0.000	0.000	1.958	0.000	0.000	0.000	0.000
2.4-Dimethylphenylacetic acid	0.000	0.000	2.874	0.000	0.000	0.000	0.000
Chrysanthenone	0.000	0.000	4.210	0.000	0.000	0.000	0.000
Bisabolone (6S, 7R)	0.000	0.000	2.257	1.018	0.000	0.000	0.000
1R-α-Pinene	0.000	0.000	4.337	0.000	0.000	0.000	0.000
Myrcenone	0.000	0.000	2.613	0.000	0.000	0.000	0.000
Iso-pinocamphyl angelate	0.000	0.000	2.157	0.000	0.000	0.000	0.000
α-Tumerone	0.000	0.000	0.000	1.839	0.000	29.990	34.265

After completing the PCA analysis, the next step involved analyzing PLS-DA using a predetermined model. Fig. 5 shows the results of the PLS-DA analysis, with an R^2 value of 1 and a Q^2 value of 0.998, which developed using four latent variables. The high R^2Y values (close to 1) indicated the model's fitness, whereas the high Q^2 value (>0.50) showed the model's predictability [16, 17]. The PLS-DA score plot describes TEO grouping into Highland and Lowland origin. The PLS models were validated using the permutation test to confirm the validity and avoid over-prediction of the developed models. The model was validated by determining R^2Y and Q^2 using a permutation test Q^2 between the actual and permuted values (fig. 6b). A model is considered valid when all R^2 -values and Q^2 -values on the left are lower in the permutation plot than the actual points

on the right [16]. This study performed the permutation test 20 times, revealing that the original model was valid and reliable in explaining and predicting X and Y matrix variations. The loading column plot was developed to identify the correlation between the growing location and the chemical constituents (fig. 6a). The bars above zero (0) point show metabolite which significantly influences the classification of the growing location. Different metabolites contributing to the correlation were distinguished using the variable importance for the projection (VIP) value. Metabolites with a VIP greater than one ($VIP > 1.0$) were considered significant. The two most influential metabolites for determining growing location were α-phellandrene and D-limonene (fig. 7).

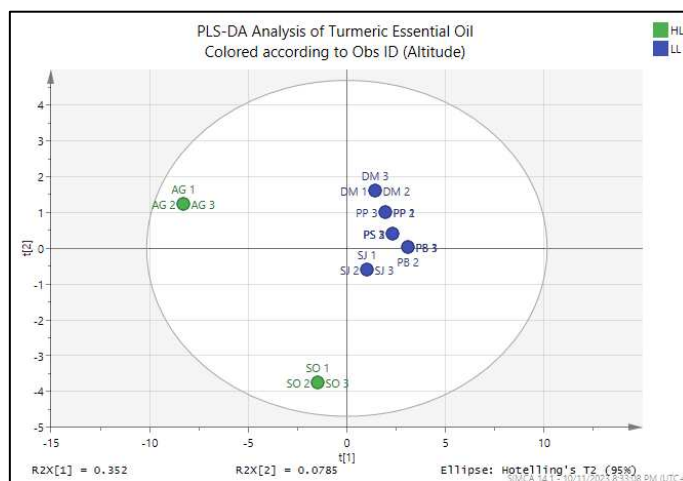


Fig. 5: PLS-DA score plots of turmeric essential oils

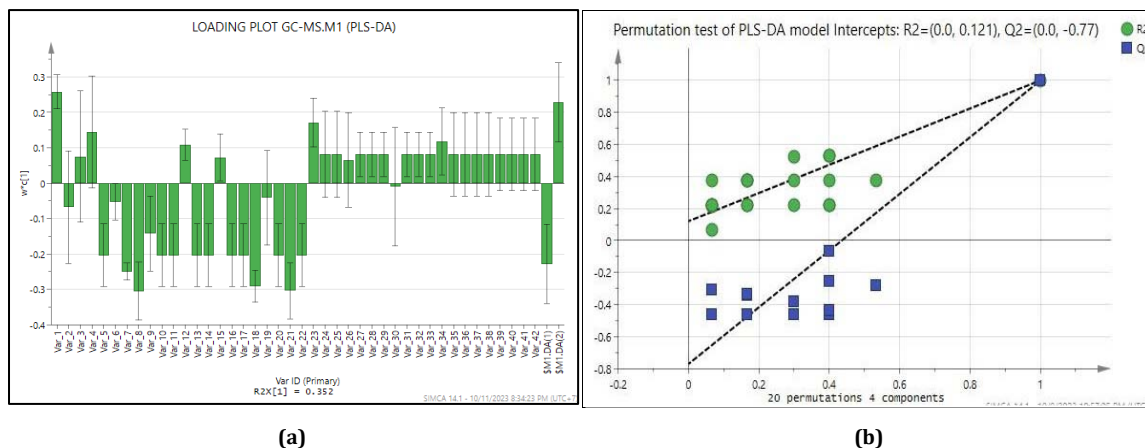


Fig. 6: (a) PLS-DA loading plot of TEO; (b) The permutation test of PLS-DA model

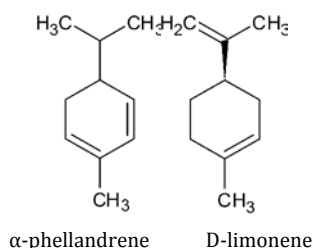


Fig. 7: The influential metabolites for determining growing location

The variations in the chemical composition of EOs are greatly affected by environmental conditions, including geographic variation and climate. Altitudinal change has a significant impact on terrestrial ecosystems as a result. A considerable difference in altitude can result in simultaneous changes in relative humidity, wind velocity, water level, temperature, and radiation rate. As a

result, environmental alterations can influence a wide range of eco-physiological responses in plant bodies [18, 19].

Promoting of fibroblast cell proliferation

Turmeric EOs and positive control (curcumin) promoted the proliferation of fibroblast cells, as shown in fig. 8. The highest fibroblast cell proliferation was demonstrated by turmeric essential oil originating from the Padang Pariaman area, with a percentage of 116% at a concentration of 1 µg/ml. Turmeric essential oil at a 100 µg/ml concentration showed toxicity to fibroblast cells where the percentage of cell proliferation was below 85%, except for TEO from Padang Pariaman and Sijunjung essential oils, which showed cell proliferation percentages of 89.51% and 92.02%. On the contrary, at lower concentrations (0.1, 1, and 10 µg/ml). TEO from Sijunjung, Padang Pariaman, and Pesisir Selatan showed an increase in fibroblast cell proliferation to above 99%. It happened may be due to a receptor-based mechanism of action. High doses of essential oils can saturate or toxicate the receptors so that higher doses are ineffective. However, the growing location of TEO did not affect the fibroblast cells proliferation (p>0.05).

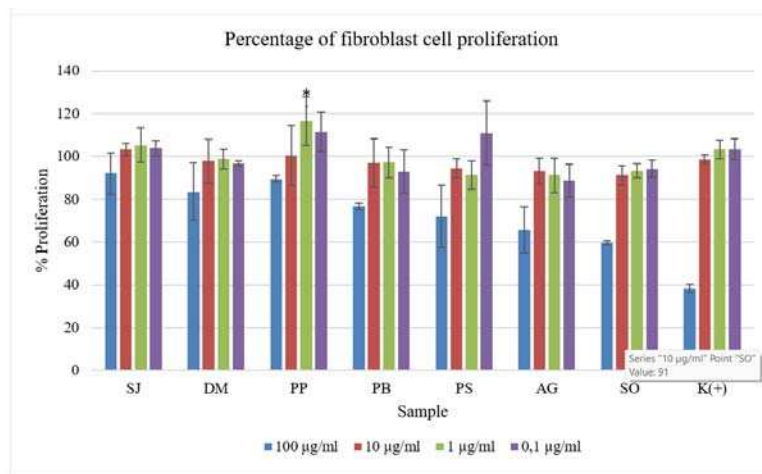


Fig. 8: Percentage of fibroblast cell proliferation after treating with TEO and curcumin K(+) mean curcumin; *) means that have significant different with positive control (p<0.05)

Migration of fibroblast cells

TEO was further evaluated for its capability to trigger the migration of fibroblast cells. Confluent fibroblast monolayers were scratched. Turmeric essential oil (0.1, 1, and 10 µg/ml) was added to the scratches. The progress of the scratch closure was monitored at 24 and 48 h. The results of the wound closure

percentage are illustrated in fig. 9 and fig. 10. The findings indicated that there were significant different (p<0.05) in the wound closure percentage for all TEOs at a concentration of 0.1µg/ml when compared to the control (without any samples) after 48 h of incubation. Moreover, at a concentration of 1µg/ml, there were significant differences between all samples except those from Pesisir Selatan and the control (without samples). At a

10 µg/ml concentration, there was a significant difference between samples from Padang Pariaman, Sijunjung and West Pasaman with the control (without sample). The positive control (curcumin) showed have no significant difference at any

concentrations with the control (without sample). These results were in accordance with previous research, where by candelula extract at low concentrations showed a higher percentage of wound closure than high concentrations [20].

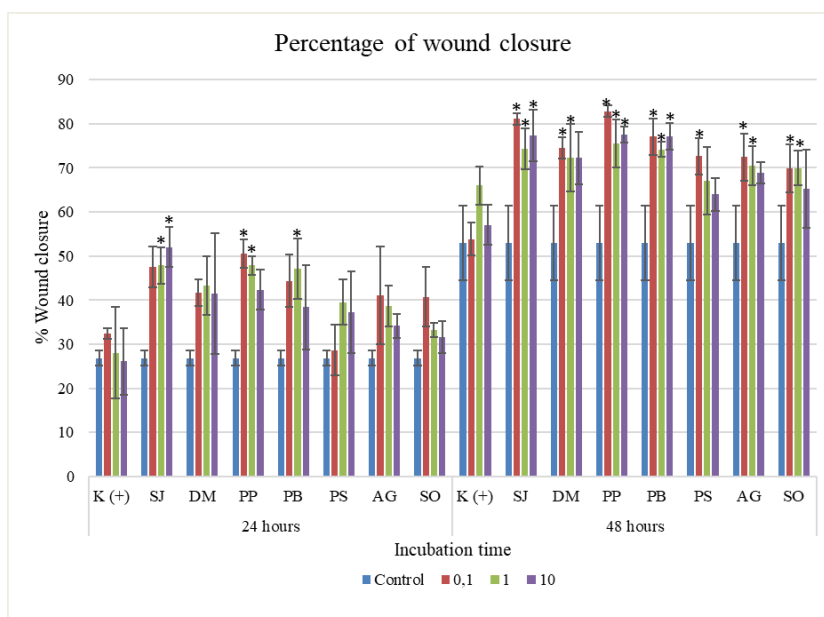


Fig. 9: Percentage of wound closure after treating with TEO and curcumin, K(+) mean curcumin; *) means that have significant different with positive control (p<0.05)

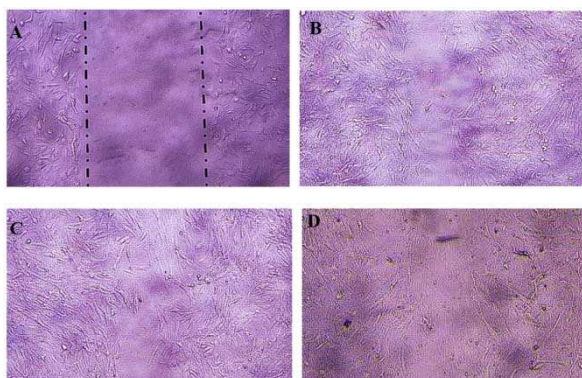


Fig. 10: Illustration of wound closure (A) Negative control (without any samples) at 0 h (B) Negative control (without any samples) at 24 h (C) Fibroblast cells with 10 µg/ml TEO after 48 h (D) Fibroblast cells with 10 µg/ml curcumin after 48 h

Plant extracts were evaluated for their ability to promote wound healing using two key parameters: closure time and contraction [21]. The biological activities of essential oils (EOs) are attributed to the compounds that make up their chemical composition. EOs comprise terpenoids, which have been demonstrated to enhance wound healing by promoting wound contraction and increasing epithelialization rates through their astringent and antimicrobial properties [7]. Eucalyptol (1,8-cineole) plays a crucial role in ulcer healing and exhibits gastroprotective effects [22].

CONCLUSION

The combination of FTIR spectral fingerprint patterns with chemometric analysis could be able to classify TEO based on the altitude of the growing location. The GC-MS spectra combined with chemometrics can identify the metabolite responsible for the determination. Turmeric essential oil showed the potential to develop as a wound-healing agent. However, the growing location

did not affect the biological activity of TEO collected from different regions in West Sumatra.

ACKNOWLEDGEMENT

Authors would like to thank to Faculty of Pharmacy Universitas Andalas for funding this research.

FUNDING

Faculty of Pharmacy Andalas University (Indonesia) through Fundamental Research Grant No.02/UN16.10. D/PJ.01./2023

AUTHORS CONTRIBUTIONS

Suryati Syafri: Methodology, Writing-Original Draft, Writing-Review and Editing; Riskana Soraya Putri: Methodology, Writing-Original Draft, Syofyan: Supervision, Methodology, Review and Editing; Yohanes Allen: Supervision, Review and Editing; Dachriyanus: Supervision, Resources, Funding acquisition, Review and Editing; Irwandi Jaswir: Supervision, Resources, Funding acquisition, Review and Editing, Faridah Yusof: Supervision, Resources, Funding acquisition, Review and Editing.

CONFLICT OF INTERESTS

Authors state no conflict of interest.

REFERENCES

- Cheppudira B, Fowler M, McGhee L, Greer A, Mares A, Petz L. Curcumin: a novel therapeutic for burn pain and wound healing. *Expert Opin Investig Drugs*. 2013;22(10):1295-303. doi: 10.1517/13543784.2013.825249, PMID 23902423.
- Hamm RL. Drug-hypersensitivity syndrome: diagnosis and treatment. *J Am Coll Clin Wound Spec*. 2011;3(4):77-81. doi: 10.1016/j.jcws.2012.06.001, PMID 24527369.
- Shetty V, Schwartz HC. Wound healing and perioperative care. *Oral Maxillofac Surg Clin North Am*. 2006;18(1):107-13. doi: 10.1016/j.coms.2005.09.004, PMID 18088815.
- Addis R, Cruciani S, Santaniello S, Bellu E, Sarais G, Ventura C. Fibroblast proliferation and migration in wound healing by

- phytochemicals: evidence for a novel synergic outcome. *Int J Med Sci.* 2020;17(8):1030-42. doi: 10.7150/ijms.43986, PMID 32410832.
5. Syafri S, Husni E, Wafiqah N, Ramadhan F, Ramadani S, Hamidi D. Evaluation of antimicrobial and proliferation of fibroblast cells activities of citrus essential oils. *Open Access Maced J Med Sci.* 2022;10(A):1051-7. doi: 10.3889/oamjms.2022.8596.
 6. Costa MF, Durço AO, Rabelo TK, de Barreto RSS, Guimarães AG. Effects of carvacrol, thymol and essential oils containing such monoterpenes on wound healing: a systematic review. *J Pharm Pharmacol.* 2019;71(2):141-55. doi: 10.1111/jphp.13054, PMID 30537169.
 7. Komakech R, Matsabisa MG, Kang Y. The wound healing potential of *Aspilia africana* (Pers.) C.D. adams (Asteraceae). *Evidence-Based Complementary and Alternative Medicine.* 2019;2019:1-12. doi: 10.1155/2019/7957860.
 8. Barra A. Factors affecting chemical variability of essential oils: a review of recent developments. *Nat Prod Commun.* 2009;4(8):1147-54. doi: 10.1177/1934578X0900400827, PMID 19769002.
 9. Diliarosta S, Prima Sari M, Ramadhani R, Efendi A. We are Intech open, the world's leading publisher of open-access books built by scientists for scientists TOP 1 %. *Intech.* 2016;13.
 10. Arbain D. Inventory, constituents and conservation of biologically important Sumatran plants. *Nat Prod Commun.* 2012;7(6):799-806. doi: 10.1177/1934578X1200700627, PMID 22816311.
 11. Ziaee M, Khorrami A, Ebrahimi M, Nourafcan H, Amiraslazadeh M, Rameshrad M. Cardioprotective effects of essential oil of *Lavandula angustifolia* on isoproterenol-induced acute myocardial infarction in rat. *Iran J Pharm Res.* 2015;14(1):279-89. PMID 25561934.
 12. Fahmi Z, Mudasir M, Rohman A. Attenuated total reflectance-FTIR spectra combined with multivariate calibration and discrimination analysis for analysis of patchouli oil adulteration. *Indones J Chem.* 2020;20(1):1-8. doi: 10.22146/ijc.36955.
 13. Rohman A, Sudjadi, Devi RD, Ramadhani D, Nugroho A. Analysis of curcumin in *Curcuma longa* and *Curcuma xanthorrhiza* using FTIR spectroscopy and chemometrics. *Res J Med Plants.* 2015;9(4):179-86. doi: 10.3923/rjmp.2015.179.186.
 14. Rohaeti E, Rafi M, Syafitri UD, Heryanto R. Fourier transform infrared spectroscopy combined with chemometrics for discrimination of *Curcuma longa*, *curcuma xanthorrhiza* and *Zingiber cassumunar*. *Spectrochim Acta A Mol Biomol Spectrosc.* 2015;137:1244-9. doi: 10.1016/j.saa.2014.08.139, PMID 25305617.
 15. Widawati M, Nurjana MA, Mayasari R. Perbedaan dataran tinggi dan dataran rendah terhadap keberagaman spesies anopheles spp. di provinsi nusa tenggara timur. *Aspirator J Vector Borne Dis Stud.* 2018;10(2):103-10. doi: 10.22435/asp.v10i2.206.
 16. Maree J, Kamatou G, Gibbons S, Viljoen A, Van Vuuren S. The application of GC-MS combined with chemometrics for the identification of antimicrobial compounds from selected commercial essential oils. *Chemom Intell Lab Syst.* 2014;130:172-81. doi: 10.1016/j.chemolab.2013.11.004.
 17. Windarsih A, Nisa K, Indrianingih AW, Darsih C, Handayani S, Wulanjati MP. The use of ¹H-NMR spectroscopy and chemometrics of pattern recognition for authentication of *Curcuma xanthorrhiza* adulterated with *Zingiber montanum*. *IOP Conf Ser: Mater Sci Eng.* 2021;1011(1):1-7. doi: 10.1088/1757-899X/1011/1/012050.
 18. Jugreet BS, Suroowan S, Rengasamy RRR, Mahomoodally MF. Chemistry, bioactivities, mode of action and industrial applications of essential oils. *Trends Food Sci Technol.* 2020;101:89-105. doi: 10.1016/j.tifs.2020.04.025.
 19. Figueiredo AC, Barroso JG, Pedro LG, Scheffer JJC. Factors affecting secondary metabolite production in plants: volatile components and essential oils. *Flavour & Fragrance J.* 2008;23(4):213-26. doi: 10.1002/ffj.1875.
 20. Fronza M, Heinzmann B, Hamburger M, Laufer S, Merfort I. Determination of the wound healing effect of calendula extracts using the scratch assay with 3T3 fibroblasts. *J Ethnopharmacol.* 2009;126(3):463-7. doi: 10.1016/j.jep.2009.09.014, PMID 19781615.
 21. Juneja K, Mishra R, Chauhan S, Gupta S, Roy P, Sircar D. Metabolite profiling and wound-healing activity of *Boerhavia diffusa* leaf extracts using *in vitro* and *in vivo* models. *J Tradit Complement Med.* 2020;10(1):52-9. doi: 10.1016/j.jtcme.2019.02.002, PMID 31956558.
 22. Freire G, Caldas R, Rodrigo A, Araujo AV, Sette S, Lafayette L. Gastroprotective mechanisms of the monoterpene 1, 8-cineole (eucalyptol); 2015.